RSC Advances

COMMUNICATION

View Article Online
View Journal | View Issue

Cite this: *RSC Adv.*, 2015, **5**, 45688

Received 25th April 2015
Accepted 15th May 2015

DOI: 10.1039/c5ra07513k

www.rsc.org/advances

Ultra-high uptake and selective adsorption of organic dyes with a novel polyoxomolybdate-based organic–inorganic hybrid compound†

Yan-Qiu Zhang,[a] Chong-Chen Wang,*[ab] Tian Zhu,[a] Peng Wang[a] and Shi-Jie Gao[a]

A novel organic–inorganic hybrid compound, $(4\text{-Hap})_4[Mo_8O_{26}]$ (4-ap = 4-aminopyridine) (**1**), was synthesized *via* a hydrothermal method, and utilized to conduct adsorptive uptake of typical organic dyes, in which some key parameters of dye adsorption were investigated. The results revealed that compound **1** demonstrated rapid adsorption of methylene blue (MB) with ultra-high efficiency and capacity, as well as achieving rapid and highly selective adsorption of MB from MB/MO (MO = methyl orange) and MB/RhB (RhB = rhodamine B) mixtures.

With the rapid development of industries including medicine, textile, leather, printing, and plastic,[1] more than 100 000 commercially available dyes with over 7×10^5 t are discharged annually to the detriment of water quality worldwide.[2] Due to ecological and environmental importance, removing organic dyes with high toxicity and hard degradation from wastewater has become a hot research topic. Furthermore, considering sustainable development, it is extremely desirable to recover and re-use the enriched organic dyes if they could be selectively separated from their mixtures. Various methods have been used for removing/treating and recovering organics dyes in wastewater. Among these technologies, adsorption has been given growing interest owning to their low cost, high efficiency, and ease of operation.[3] Thus, it is indispensable to explore new adsorbents with ultra-high adsorption efficiency and capacity towards dyes, as well as highly selective ability to separate different organic dyes from their mixtures.[4] Multifunctional organic–inorganic hybrid crystalline materials, which assembly molecular components into periodic framework, have captured considerable attentions owing to their diverse and easily tailored structures,[5] and their various potential applications in catalysis,[6,7] separation,[8–10] gas storage,[7,11,12] carbon dioxide capture,[13,14] photocatalysis,[2,15] and so on.[9,16–18] Very recently, some ionic hybrid crystalline materials were also used for selectively adsorbing and further separating cationic or anionic dye molecules from mixed dyes solution by host–guest electronic interactions and/or guest–guest exchange interactions,[4,19–31] but still facing the challenges of either time consume or operating in non-aqueous solutions.[22,24–26] In this paper, a novel organic–inorganic hybrid crystalline material, $(4\text{-Hap})_4[Mo_8O_{26}]$ (**1**) was synthesized, which can rapidly and efficiently adsorb methylene blue (MB) as well as selectively uptake MB from the MB/MO and MB/RhB aqueous solution, respectively.

White block-like crystal, $(4\text{-Hap})_4[Mo_8O_{26}]$ (FM: $C_{20}H_{28}Mo_8N_8O_{26}$) (**1**) were obtained from the mixture of $CdCl_2 \cdot 2.5H_2O$, ammonium molybdate tetrahydrate and 4-aminopyridine (4-ap) under hydrothermal conditions for 72 h. Finally, they were isolated and washed with deionized water and ethanol. Single crystal X-ray diffraction analysis revealed that compound **1** crystallizes in triclinic, space group $P\bar{1}$, (CCDC 1055385, and details of X-ray data collection and refinement for **1** are listed in Table S1, ESI†), and the structure of **1** contains one discrete β-octamolybdate anion $[Mo_8O_{26}]^{4-}$ and four discrete protonated 4-aminopyridinium ions, as illustrated in Fig. 1(a). Each $[Mo_8O_{26}]^{4-}$ polyanion is built up from eight distorted MoO_6 octahedral units by sharing edges and corners with local C_{2h} symmetry. Eight molybdenum atoms can be visualized as an edge-sharing double O-centred trigonal bipyramid. The overall dimensions of the octamolybdate polyanion in **1** are consistent with those reported compounds containing the same type polyanion,[32,33] in spite of slightly difference in Mo–O bond lengths due to the different interactions between cationic units and polyanionic units (the selected bond lengths and angles for **1** are listed in Table S2, ESI†). The basic structural unit of **1** consists of a dissociative unit $[Mo_8O_{26}]^{4-}$, which is much different with the infinite

[a]*Beijing Engineering Research Center of Sustainable Urban Sewage System Construction and Risk Control, Beijing University of Civil Engineering and Architecture, Beijing, 100044, China. E-mail: chongchenwang@126.com; Fax: +86 10 68322123*

[b]*Key Laboratory of Urban Stormwater System and Water Environment (Ministry of Education), Beijing University of Civil Engineering and Architecture, Beijing, 100044, China*

† Electronic supplementary information (ESI) available: Crystallographic data, SEM image, UV-vis DRS, adsorption parameters and photo of SPE setup. CCDC 1055385. For ESI and crystallographic data in CIF or other electronic format see DOI: 10.1039/c5ra07513k

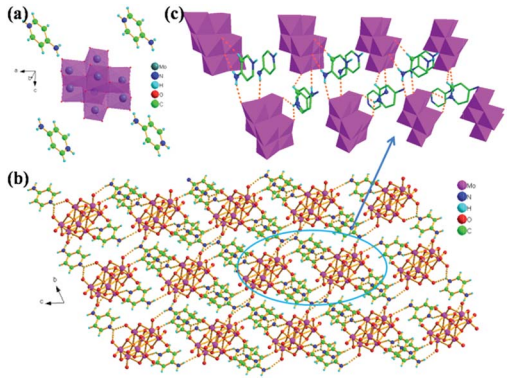

Fig. 1 (a) The asymmetric unit of structure of compound **1**. (b) View of the 3D structure built up with hydrogen-bonding interactions of **1**. (c) Detailed hydrogen-bonding interactions in compound **1**.

$[Mo_8O_{26}]_n^{4n-}$ chains in $(4\text{-Hap})_{4n}[Mo_8O_{26}]_n$, a compound with similar structure.[34] Each 4-aminopyridine molecule is protonated at nitrogen atom position of the pyridine ring, which is further linked to $[Mo_8O_{26}]^{4-}$ to construct a 3D framework *via* strong hydrogen bonds (N–H···O) (Table S3, ESI†), and also acts as counter-ion to compensate the anionic charge of $[Mo_8O_{26}]^{4-}$ polyanion,[35] as illustrated in Fig. 1(b) and (c).

To characterize the phrase purity of **1**, powder X-ray diffraction (PXRD) has been checked at ambient temperature. The results revealed that the measured PXRD patterns of **1** matched well with those simulated patterns derived from the single-crystal X-ray diffraction data, indicating high phrase purity of **1** (as shown in Fig. 2(a)). Furthermore, the thermal gravimetric analysis (TGA) was investigated under air atmosphere, and the TGA curve of **1** revealed that **1** is stable up to 300 °C, as illustrated in Fig. 2(c). The surface charge of the particles was assessed by zeta potential measurements with the result of −46.7 mV, implying that the surface of **1** is much negative.[36]

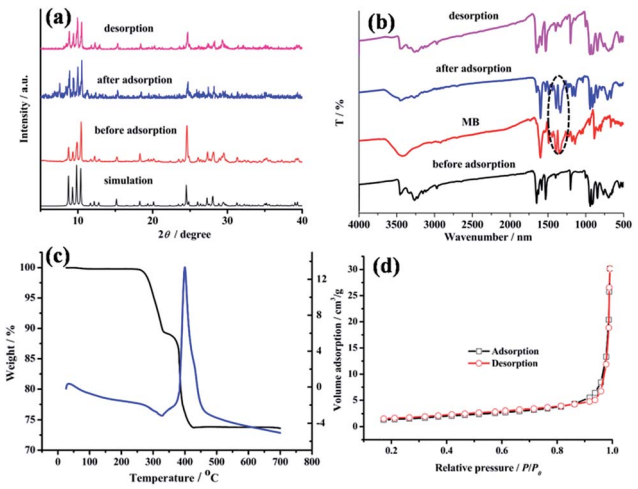

Fig. 2 (a) Comparison of XRD patterns of the simulated one from single crystal data, compound **1** before and after adsorption, and compound **1** after desorption. (b) FTIR spectra of as-synthesized **1**, **1** after absorbing MB, MB dye and **1** after desorption. (c) TGA curve of **1**. (d) N_2 adsorption–desorption isotherms of **1**.

To further evaluate the adsorption activity on organic pollutants of **1**, cationic methylene blue (MB), cationic rhodamine B (RhB) and anionic methylene orange (MO) were selected as targets to conduct adsorption process, considering that both the charge and size of organic dyes are the most important factors controlling the adsorption process,[37] and the detailed experimental process is described in the ESI.† As illustrated in Fig. 3, the adsorption ability of **1** was different towards MB, RhB and MO with identical initial concentration (10 mg L^{-1}). The removal percent of MB can be achieved at 100% in 120 min, while only 47.5% and 9.0% of RhB and MO can be removed up to 120 min, respectively. In fact, the process of MB adsorption onto **1** was rapid, in which *ca.* 53.9% MB can be removed in 10 min. To better understand adsorption ability of **1**, MB was chosen as the removal target to study the adsorption performance of **1** in detail, including adsorption kinetic parameters, isotherm modes, and thermodynamic parameters. The effects of contact time (t) on the adsorption amount and removal percentage of MB by **1** are shown in Fig. S3 (ESI†). The adsorption amount (q_t) of MB by **1** was found to increase with t and initial concentration (C_0), which also illustrated the favourable adsorption at high dye concentrations. There was a rapid uptake of MB at the initial period, which was possibly due to that a large number of vacant adsorption sites are available for adsorption at initial period[38,39] and the high affinity between MB molecules and the surface of **1**.[38,39] Finally, the colour of MB in aqueous cannot be detected by naked eye with different initial concentration of MB and different added amount of **1**. Compound **1** exhibited the maximum adsorption capacity of 916.04 mg MB per gram when it was soaked in 500 mg L^{-1} MB aqueous solution for 10 h, which is much higher than those previously reported adsorbents, as listed in Table 1. Previous studies have illuminated that the surface area is an important factor to influence the adsorption capacity.[40,41] While **1** possesses inferior surface area (5.17 m^2 g^{-1}) determined by N_2 sorption, but has a strong affinity in binding MB, indicating the poor porosity of **1** prevents N_2 sorption, but

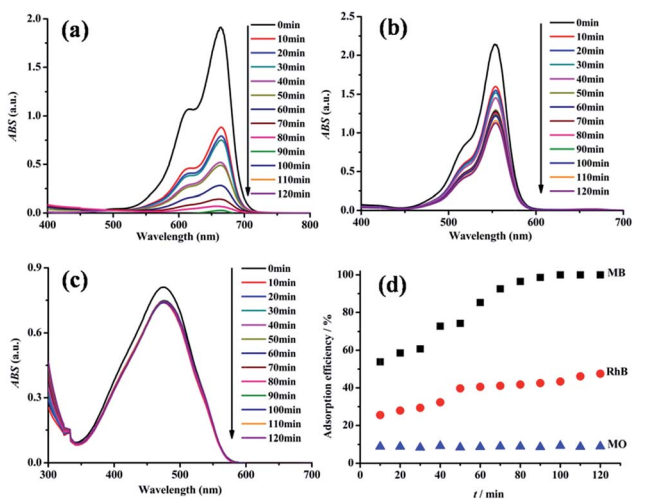

Fig. 3 The adsorption capability of **1** toward different dyes: (a) MB; (b) RhB; (c) MO. (d) The removal efficiency of MB, RhB, and MO, respectively.

Table 1 Comparison of the adsorption capacities of MB onto some typical adsorbents

Adsorption	Adsorption capacity (mg g^{-1})	Ref.
1	916.04	This work
$H_3PW_{12}O_4$@ZIF-8	810	45
Compound A[a]	708	20
Compound B[b]	725	20
CNTs-A	400	38
$PW_{11}V$@MIL-101	371	19
Active carbon	238	46
MOF-235	187	47
Carbon nanotubes	46.2	48
Graphene	153.83	49
Graphene oxide	144.92	50
GO/CA[c]	188.81	50

[a] Compound A = $[(CH_3)_2NH_2]_6[M(H_2O)_6]_3[M_6(\eta^6\text{-TATAT})_4(H_2O)_{12}]\cdot xH_2O$ (M = Co^{2+}, x = 6). [b] Compound B = $[(CH_3)_2NH_2]_6[M(H_2O)_6]_3[M_6(\eta^6\text{-TATAT})_4(H_2O)_{12}]\cdot xH_2O$ (M = Ni^{2+}, x = 6). [c] CA = calcium alginate immobilized graphene oxide.

do not impede dye uptake from solution.[42] Hence, it can also be concluded that the external surface area here is not the exclusive factor to determine the adsorption capacity.[23] And it is worthy to noting that compound **1** does not need any activation process, being quite different from other reported counter partners for dyes sorption.[43,44]

In order to clarify the characteristics of the adsorption process, the changes of adsorbed amount with time are fitted with pseudo-first-order and pseudo-second-order kinetic, respectively.[51–53] The calculated kinetic constants (k_1, k_2) and the corresponding correlation coefficients (R^2) of the pseudo-first-order and pseudo-second-order kinetic are shown in Table S4 (ESI†) for C_0 (MB) = 30, 50, 100 mg L^{-1}. It is clear that the pseudo-second-order model is more suitable for the adsorption of MB by **1** because of their relatively high R^2 values (0.978, 0.951 and 0.991 for C_0 (MB) = 30, 50, 100 mg L^{-1}, respectively). From Table S4 (ESI†), the pseudo-second-order constants (k_2) decrease with the increase of initial MB concentration, which can be explained that the competition of MB binding with the surface active sites will be fierce at higher concentrations, resulting in lower sorption rates.[54,55] Furthermore, the k_2 for adsorbing MB on **1** is much larger than those of MOF-235 and activated carbon with the same concentration of MB (30 mg L^{-1})[47] in previous reports, indicating more rapid adsorption of MB on **1**. The calculated q_e values (54.3 mg g^{-1}, 107.5 mg g^{-1} and 158.7 mg g^{-1} for C_0 (MB) = 30, 50, 100 mg L^{-1}, respectively) from pseudo-second-order model are consistent with the experimental values (51.03 mg g^{-1}, 99.76 mg g^{-1} and 156.90 mg g^{-1}, respectively), as listed in Table S4 (ESI†).

In order to describe the equilibrium isotherms, the equilibrium data of MB absorbing onto **1** were fitted with Langmuir, Freundlich, and Dubinin–Radushkevich (D–R), respectively. As shown in Table S5 (ESI†), Langmuir isotherm model preferred to describe the adsorption process.[56–59] The values of ΔG° (Table S6, ESI†) were found to decrease from −31.33 to −35.94 kJ mol^{-1} with the increase of temperature, indicating that the adsorption

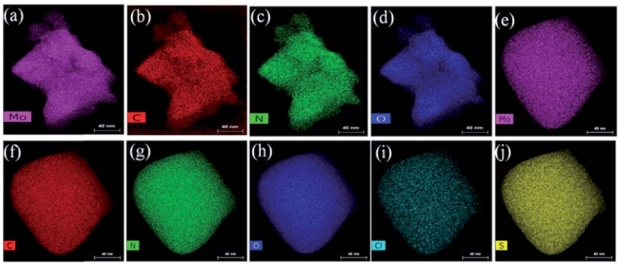

Fig. 4 (a)–(d) Mo, C, N, and O elemental maps of compound **1**, (e)–(j) Mo, C, N, O, Cl, and S elemental maps of compound **1** after adsorption.

process of MB on **1** becomes more favourable at higher temperatures,[60] which can also be certified from maximum adsorption amount increase from 496.1 mg g^{-1} at 298 °C to 680.3 mg g^{-1} at 318 °C. The negative values of ΔG° suggested that the sorption process may be controlled by mainly physical sorption and partially chemical sorption.[61] The positive value of ΔH° (37.40 kJ mol^{-1}) indicated that the adsorption reaction is endothermic, and the positive value of ΔS° (230.77 J mol^{-1} K^{-1}) implied the increase randomness at the solid–solution interface during the adsorption of MB onto **1**.

In addition, the patterns of XRD of **1** after adsorption matched well with the patterns of **1** as prepared, as depicted in Fig. 2(a), indicating good stability of crystalline sample **1** after adsorption. Although there were no evident changes on **1** after adsorption, the elemental mapping obtained from TEM revealed the existence of Cl and S (two characteristic elements of MB) in **1** after adsorbing MB, besides of Mo, C, N and O in **1** as-prepared, as illustrated in Fig. 4. The adsorption of MB onto **1** was affirmed by XPS and FTIR, which confirmed the strong signals of S element in the XPS patterns (Fig. 5) and the characteristics peaks of MB in FTIR spectra (Fig. 2(b)).

The selective adsorption of dyes is more attractive and challenging. In this paper, cationic MB (molecule size 1.38 nm × 0.64 nm × 0.21 nm), cationic RhB (molecule size 1.56 nm × 1.35 nm × 0.42 nm) and anionic MO (molecule size 1.54 nm × 0.48 nm × 0.28 nm) were selected, considering that they possess different sizes and different charges. The selective uptake of dyes was tested using the MB/MO mixture (200 mL, $C_{MB} = C_{MO}$ = 10 mg L^{-1}) and MB/RhB mixture (200 mL, $C_{MB} = C_{RhB}$ = 10 mg L^{-1}) with 0.05 g **1** as absorbent, and then the process was monitored by UV-vis spectroscopy. As MB and MO are similar in molecule size, the preferable uptake of MB from

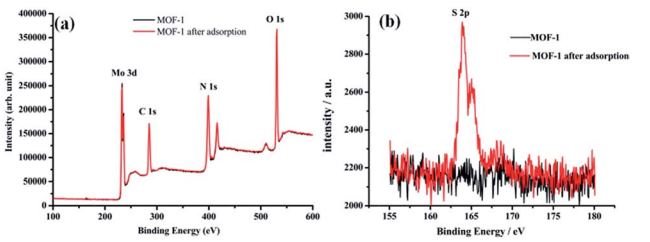

Fig. 5 (a) XPS wide scans spectra of compound **1** before and after MB adsorption. (b) XPS spectra for S 2p regions of compound **1** before and after MB adsorption.

MB/MO mixture may be assigned to the anionic nature of **1**, as shown in Fig. 6(a). For comparison, cationic RhB was selected to mix with cationic MB, and the results revealed that MB was also preferably adsorbed on **1** from the MB/RhB mixture (as illustrated in Fig. 6(b)), which may imply that the uptake of dyes is heavily influenced by molecule size along with charges.[36]

Furthermore, its potential application was tested by solid phase extraction (SPE) column, in which the Agilent Bond Elut C18 in the original column was replaced by 0.90 g compound **1** (particle size of 0.1 mm) with 5 mm packing height. The MB/MO mixture (32 mL, $C_{MB} = C_{MO} = 10$ mg L^{-1}) solution was pumped *via* automatic vacuum through the column with the flow rate 4 mL min^{-1} (Fig. S4, ESI†). The orange MO was passed through the SPE column directly and rapidly, while the MB was retained in **1** as column packing. In order to qualify the removal efficiency, the UV-vis absorbance was introduced to determine the MB concentration of the effluent through the column, and the results showed that the removal efficiency of MB can achieve 100%, while the concentration of MO only had a little drop with the removal percentage of *ca.* 5.7%, implying rapid and highly efficient separation of MB and MO from their mixture due to highly selective uptake of MB. In order to determine the stability and re-usage of the SPE column, the SPE column was back-flushed with methanol for 4 h, After back-flushing, the column was reused in another 6 circles with identically high separation efficiency, demonstrating **1** possessing good reusability and potential of practical application. The stability of the packing in the column was confirmed by XRD, FTIR and SEM, as shown in Fig. 1(a) and (b) and Fig. S1 (ESI†), respectively.

In summary, a novel organic–inorganic hybrid material named $(4\text{-Hap})_4[Mo_8O_{26}]$ (**1**) was synthesized under hydrothermal conditions. Compound **1** exhibited ultra-high uptake efficiency and capacity to MB, and the adsorption process followed pseudo-second-order kinetic model as well as Langmuir isotherms. The adsorption of MB onto **1** at various temperatures showed that the adsorption is spontaneous (negative ΔG°), endothermic (positive ΔH°) and the randomness increases (positive ΔS°) with the adsorption process. Compound **1** also preferred to uptake MB from MB/MO mixture and MB/RhB mixture, which encourage us to prepare SPE column with **1** as filler packing. Our self-made SPE column can achieve rapid and efficiently separation of MB and MO from their mixture, which also exhibit excellent stability. Further researches should be carried out to clarify the adsorptive activities on other organic pollutants.

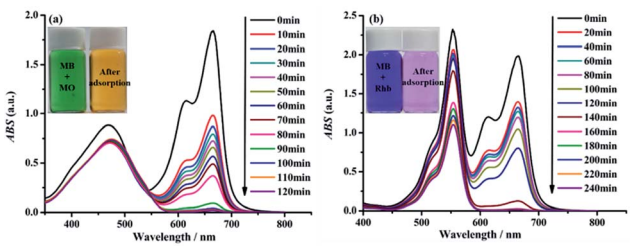

Fig. 6 The selective adsorption capacity of **1** toward the mixed dyes of (a) MB/MO and (b) MB/RhB.

Acknowledgements

We thank the financial support from the Beijing Natural Science Foundation & Scientific Research Key Program of Beijing Municipal Commission of Education (KZ201410016018), the Training Program Foundation for the Beijing Municipal Excellent Talents (2013D005017000004), the Importation & Development of High-Caliber Talents Project of Beijing Municipal Institutions (CIT&CD201404076), Special Fund for Cultivation and Development Project of the Scientific and Technical Innovation Base (Z141109004414087).

Notes and references

1 G. Crini, *Bioresour. Technol.*, 2006, **97**, 1061.
2 C.-C. Wang, J.-R. Li, X.-L. Lv, Y.-Q. Zhang and G. Guo, *Energy Environ. Sci.*, 2014, **7**, 2831.
3 N. A. Khan, Z. Hasan and S. H. Jhung, *J. Hazard. Mater.*, 2013, **244**, 444.
4 H. He, C.-C. Wang, J. Yang, W.-Q. Kan, H.-M. Zhang, Y.-Y. Liu and J.-F. Ma, *J. Mater. Chem. A*, 2015, **3**, 1675.
5 J. J. Perry IV, J. A. Perman and M. J. Zaworotko, *Chem. Soc. Rev.*, 2009, **38**, 1400.
6 J. Lee, O. K. Farha, J. Roberts, K. A. Scheidt, S. T. Nguyen and J. T. Hupp, *Chem. Soc. Rev.*, 2009, **38**, 1450.
7 R. J. Kuppler, D. J. Timmons, Q.-R. Fang, J.-R. Li, T. A. Makal, M. D. Young, D. Yuan, D. Zhao, W. Zhuang and H.-C. Zhou, *Coord. Chem. Rev.*, 2009, **253**, 3042.
8 J.-R. Li, J. Sculley and H.-C. Zhou, *Chem. Rev.*, 2011, **112**, 869.
9 J.-R. Li and H.-C. Zhou, *Nat. Chem.*, 2010, **2**, 893.
10 J.-R. Li, R. J. Kuppler and H.-C. Zhou, *Chem. Soc. Rev.*, 2009, **38**, 1477.
11 N. L. Rosi, J. Eckert, M. Eddaoudi, D. T. Vodak, J. Kim, M. O'Keeffe and O. M. Yaghi, *Science*, 2003, **300**, 1127.
12 S. Ma and H.-C. Zhou, *Chem. Commun.*, 2010, **46**, 44.
13 K. Sumida, D. L. Rogow, J. A. Mason, T. M. McDonald, E. D. Bloch, Z. R. Herm, T.-H. Bae and J. R. Long, *Chem. Rev.*, 2011, **112**, 724.
14 J. M. Simmons, H. Wu, W. Zhou and T. Yildirim, *Energy Environ. Sci.*, 2011, **4**, 2177.
15 H.-P. Jing, C.-C. Wang, Y.-W. Zhang, P. Wang and R. Li, *RSC Adv.*, 2014, **4**, 54454.
16 Y. Xiong, F. Ye, C. Zhang, S. Shen, L. Su and S. Zhao, *RSC Adv.*, 2015, **5**, 5164.
17 T. A. Vu, G. H. Le, C. D. Dao, L. Q. Dang, K. T. Nguyen, Q. K. Nguyen, P. T. Dang, H. T. K. Tran, Q. T. Duong, T. V. Nguyen and G. D. Lee, *RSC Adv.*, 2015, **5**, 5261.
18 Y. Xu, J. Jin, X. Li, Y. Han, H. Meng, T. Wang and X. Zhang, *RSC Adv.*, 2015, **5**, 19199.
19 A. X. Yan, S. Yao, Y. G. Li, Z. M. Zhang, Y. Lu, W. L. Chen and E. B. Wang, *Chem.–Eur. J.*, 2014, **20**, 6927.
20 Z. Zhu, Y.-L. Bai, L. Zhang, D. Sun, J. Fang and S. Zhu, *Chem. Commun.*, 2014, **50**, 14674.
21 D.-M. Chen, W. Shi and P. Cheng, *Chem. Commun.*, 2015, **51**, 370.
22 X.-L. Lv, M. Tong, H. Huang, B. Wang, L. Gan, Q. Yang, C. Zhong and J.-R. Li, *J. Solid State Chem.*, 2015, **223**, 104.

23 Q. Chen, Q. He, M. Lv, Y. Xu, H. Yang, X. Liu and F. Wei, *Appl. Surf. Sci.*, 2015, **327**, 77.
24 L. Xiao, Y. Xiong, S. Tian, C. He, Q. Su and Z. Wen, *Chem. Eng. J.*, 2015, **265**, 157.
25 H.-N. Wang, F.-H. Liu, X.-L. Wang, K.-Z. Shao and Z.-M. Su, *J. Mater. Chem. A*, 2013, **1**, 13060.
26 Y.-C. He, J. Yang, W.-Q. Kan, H.-M. Zhang, Y.-Y. Liu and J.-F. Ma, *J. Mater. Chem. A*, 2015, **3**, 1675.
27 Y. Fan, H.-J. Liu, Y. Zhang and Y. Chen, *J. Hazard. Mater.*, 2015, **283**, 321.
28 F.-Y. Yi, W. Zhu, S. Dang, J.-P. Li, D. Wu, Y.-h. Li and Z.-M. Sun, *Chem. Commun.*, 2015, **51**, 3336.
29 Z. Hasan and S. H. Jhung, *J. Hazard. Mater.*, 2015, **283**, 329.
30 J. Huo, J. Aguilera-Sigalat, S. El-Hankari and D. Bradshaw, *Chem. Sci.*, 2015, **6**, 1938.
31 Y.-X. Tan, Y.-P. He, M. Wang and J. Zhang, *RSC Adv.*, 2014, **4**, 1480.
32 D. Attanasio, M. Bonamico, V. Fares and L. Suber, *J. Chem. Soc., Dalton Trans.*, 1992, 2523.
33 C.-C. Wang, *Z. Kristallogr. - New Cryst. Struct.*, 2006, **221**, 388.
34 J. R. Nelson, A. Narducci Sarjeant and A. J. Norquist, *Acta Crystallogr., Sect. E: Struct. Rep. Online*, 2006, **62**, m1731.
35 J. Guo, J. Yang, Y.-Y. Liu and J.-F. Ma, *Inorg. Chim. Acta*, 2013, **400**, 51.
36 A.-X. Yan, S. Yao, Y.-G. Li, Z.-M. Zhang, Y. Lu, W.-L. Chen and E.-B. Wang, *Chem.–Eur. J.*, 2014, **20**, 6927.
37 X. Zhao, X. Bu, T. Wu, S.-T. Zheng, L. Wang and P. Feng, *Nat. Commun.*, 2013, **4**, 2344.
38 J. Ma, F. Yu, L. Zhou, L. Jin, M. Yang, J. Luan, Y. Tang, H. Fan, Z. Yuan and J. Chen, *ACS Appl. Mater. Interfaces*, 2012, **4**, 5749.
39 M. Ghaedi, A. Hassanzadeh and S. N. Kokhdan, *J. Chem. Eng. Data*, 2011, **56**, 2511.
40 D.-P. Li, Y.-R. Zhang, X.-X. Zhao and B.-X. Zhao, *Chem. Eng. J.*, 2013, **232**, 425.
41 Y. Dong, B. Lu, S. Zang, J. Zhao, X. Wang and Q. Cai, *J. Chem. Technol. Biotechnol.*, 2011, **86**, 616.
42 A. S. Gupta, R. K. Deshpande, L. Liu, G. I. Waterhouse and S. G. Telfer, *CrystEngComm*, 2012, **14**, 5701.
43 E. Haque, V. Lo, A. I. Minett, A. T. Harris and T. L. Church, *J. Mater. Chem. A*, 2014, **2**, 193.
44 A. A. Adeyemo, I. O. Adeoye and O. S. Bello, *Toxicol. Environ. Chem.*, 2012, **94**, 1846.
45 R. Li, X. Ren, J. Zhao, X. Feng, X. Jiang, X. Fan, Z. Lin, X. Li, C. Hu and B. Wang, *J. Mater. Chem. A*, 2014, **2**, 2168.
46 V. Basava Rao and S. Ram Mohan Rao, *Chem. Eng. J.*, 2006, **116**, 77.
47 E. Haque, J. W. Jun and S. H. Jhung, *J. Hazard. Mater.*, 2011, **185**, 507.
48 Y. Yao, F. Xu, M. Chen, Z. Xu and Z. Zhu, *Bioresour. Technol.*, 2010, **101**, 3040.
49 T. Liu, Y. Li, Q. Du, J. Sun, Y. Jiao, G. Yang, Z. Wang, Y. Xia, W. Zhang and K. Wang, *Colloids Surf., B*, 2012, **90**, 197.
50 Y. Li, Q. Du, T. Liu, J. Sun, Y. Wang, S. Wu, Z. Wang, Y. Xia and L. Xia, *Carbohydr. Polym.*, 2013, **95**, 501.
51 B. Hameed and A. Rahman, *J. Hazard. Mater.*, 2008, **160**, 576.
52 Y.-S. Ho and G. McKay, *Process Biochem.*, 1999, **34**, 451.
53 S. Wang, H. Li and L. Xu, *J. Colloid Interface Sci.*, 2006, **295**, 71.
54 H. Chen and J. Zhao, *Adsorption*, 2009, **15**, 381.
55 A. S. Özcan, B. Erdem and A. Özcan, *Colloids Surf., A*, 2005, **266**, 73.
56 L. Ai, C. Zhang, F. Liao, Y. Wang, M. Li, L. Meng and J. Jiang, *J. Hazard. Mater.*, 2011, **198**, 282.
57 E. Eren, *J. Hazard. Mater.*, 2009, **162**, 1355.
58 N. K. Amin, *J. Hazard. Mater.*, 2009, **165**, 52.
59 Ö. Gerçel, H. F. Gerçel, A. S. Koparal and Ü. B. Öğütveren, *J. Hazard. Mater.*, 2008, **160**, 668.
60 A. Zaki, M. El-Sheikh, J. Evans and S. El-Safty, *J. Colloid Interface Sci.*, 2000, **221**, 58.
61 X.-G. Chen, S.-S. Lv, S.-T. Liu, P.-P. Zhang, A.-B. Zhang, J. Sun and Y. Ye, *Sep. Sci. Technol.*, 2012, **47**, 147.

